Chinese Journal of Chemical Engineering 90 (2026) 326–332

Contents lists available at ScienceDirect

Chinese Journal of Chemical Engineering

journal homepage: www.elsevier.com/locate/CJChE

Full Length Article

Charge transfer mediator additive facilitates uniform lithium deposition in ester-based electrolytes

Tianyi Zhou [1,*], Lin Hu [1], Qichen Lu [1], Peng Liu [1], Ruling Huang [1], Bo Hu [1], Panxing Bai [1], Shaorong Duan [1], Xiaofan Pin [1], Rong Liu [1], Kexin Zhang [1], Xiaoxu Sun [1], Yidan Wang [1], Yaoyu Li [1], Yujia Zhang [1], Yi Yan [1], Peng Jiang [2,3,*], Henghui Zhou [4,*], Xiaolong Wang [1,*]

[1] China Huaneng Clean Energy Research Institute, Future Science Park, Beijing 102209, China
[2] CAS Key Laboratory of Standardization and Measurement for Nanotechnology, CAS Center for Excellence in Nanoscience, National Center for Nanoscience and Technology, Beijing 100190, China
[3] University of Chinese Academy of Sciences, Beijing 100049, China
[4] College of Chemistry and Molecular Engineering, Peking University, Beijing 100871, China

ARTICLE INFO

Article history:
Received 26 April 2025
Received in revised form
1 July 2025
Accepted 27 September 2025
Available online 28 November 2025

Keywords:
Li metal anode
Additive
Charge transfer mediator
Li deposition
Ester-based electrolyte

ABSTRACT

The lithium redox at the Li/electrolyte interface have significantly influences on the road achieving high performance lithium metal anode (LMA). Lithium dendrite formation caused by inhomogeneous Li deposition at Li/electrolyte interface is one of the critical challenges for rechargeable Li metal batteries (LMBs). Besides, the incompatibility of commonly used commercial ester-based electrolytes with metallic lithium also limits the application of LMA, while some reported additives can only maintain their efficiency in ether-based electrolytes. In this work, 2-Mercaptopyridine (2Mpy), which we have proposed in ether-based electrolyte application, is introduced into commercial ester-based electrolyte as a redox promoter and the evolution of Li deposition and the mechanism of additive has been further investigated. The redox of Li^+/Li is accelerated and the cycling performances of LMBs in ester-based electrolyte are greatly improved with 2Mpy participated. This work further demonstrates the effectiveness of charge transfer mediator additives such as 2Mpy in ester-based electrolyte, opening up a practical path to achieving high-performance additive for lithium metal batteries.

1. Introduction

Lithium metal batteries (LMBs) based on Li metal anodes have attracted worldwide attention due to their extraordinary high theoretical energy density. However, growth of lithium dendrites still hinders the practical application of metallic lithium as anode to replace graphite anodes [1,2]. The dendrites growth is considered to be uncontrollable, result in fast electrolyte consumption and low Coulombic efficiency (CE) [3]. Worse still, lithium dendrites not only form “dead lithium” reducing the capacity of batteries, but may also penetrate the separator, causing internal short circuits or even explosions in LMBs, which is not acceptable for a commercial application [4,5]. Various strategies have been developed to suppress dendrites growth, including: (1) introducing three-dimensional current collectors or structure designing [6–9]; (2) the electrolyte engineering or adding electrolyte additives [10–14]; (3) introducing artificial protective layers [15–18]; (4) using solid state electrolyte to block Li metal dendrite growth [19–22].

In previous study, we develop a Li^+/Li redox accelerating mechanism through a charge transfer mediator additive of 2Mpy to achieve dendrite free Li metal deposition in ether-based electrolyte, which presented a novel concept for Li anodes protection [23]. A conjugated 2Mpy molecule with stable electrochemical properties, can be specifically adsorbed on Li metal surface and promote charge transfer at the Li metal/electrolyte interface. Therefore, a fast electrochemical kinetic and accelerated Li deposition can be achieved. However, the ether-based electrolytes are compatible with the Li metal and are more resistant against reduction, thus leading to a thinner SEI on the anode and higher initial Coulombic efficiency, compared with ester-based

* Corresponding authors.
E-mail addresses: ty_zhou@qny.chng.com.cn (T. Zhou), pjiang@nanoctr.cn (P. Jiang), hhzhou@pku.edu.cn (H. Zhou), xl_wang@qny.chng.com.cn (X. Wang).

https://doi.org/10.1016/j.cjche.2025.09.034

electrolytes [24]. However, ether solvents are prone to becoming oxidized when operating beyond 4.0 V (*vs* Li/Li^+), and tend to volatilize easily, complicating battery fabrication processes [25]. Therefore, although the investigation is continuous, ethers are believed to be less useful and rarely considered as electrolytes in practical application. The carbonate ester-based electrolytes, which are the most commonly used and mature electrolyte systems in commercial LIBs, are incompatible with the lithium metal anode, as the carbonate solvents (*e.g.*, ethylene carbonate, dimethyl carbonate, ethyl methyl carbonate) can be attacked and reduced readily by the electrons and then form a thick solid electrolyte interphase (SEI) layer on the Li metal [26,27]. This thick SEI slow down the diffusion of Li^+ and hinders the Li^+ desolation process during lithium plating/stripping. What's worse is that the slow migration of Li^+ can promote the growth of lithium dendrites and pose safety concerns. Therefore, investigation of the 2Mpy's effect in ester-based electrolyte still remains a significant challenge [28].

2Mpy is a promising charge transfer mediator additive for the Li^+/Li redox accelerating mechanism. Although its effects on the uniform Li deposition in ether-based electrolyte system were reported, the effectiveness of the 2Mpy's accelerating mechanism in ester-based electrolyte is still maintain uncertainty. In this paper, the behavior of 2Mpy in ester-based electrolyte during Li deposition has been further investigated. The effects of 2Mpy on the properties and morphologies of deposited Li at different current rates, and repeated plating/stripping processes have been further employed *via* several different approaches.

2. Experimental

2.1. Materials characterization

The morphology of metallic lithium anode was characterized by a scanning electron microscope (SEM, Hitachi S-4800, Japan). X-ray photoemission spectroscopy (XPS) was carried out on an Imaging Photoelectron Spectrometer (Kratos Analytical Ltd.). Before SEM or XPS testing, the electrode should be cleaned three times with DMC solvent to remove electrolyte components or lithium salt residues.

2.2. Simulation details

The DFT calculation for complexation is on the basis sets in the framework of B3LYP hybrid functional in the Dmol3 program, using Material Studio software. All the molecules were optimized using DND basis set. The SCF tolerance was 1×10^{-5} Ha (1 Ha = 27.2114 eV). The final morphology is determined by the model when the lowest total energy is reached.

2.3. Preparation of $LiFePO_4$ and NCM811 cathodes

$LiFePO_4$ (LFP) was used as cathode materials. The cathode was prepared by spreading a slurry of mixing LFP powders, carbon black and polyvinylidene fluoride (PVDF) binder (dissolved in NMP) in a mass ratio of 90:5:5 on a piece of Al foil. Then the Al foil was dried under vacuum at 120 °C for 12 h. The loading of LFP is ~8.0 $mg \cdot cm^{-2}$.

NCM811 was used as cathode materials. The cathode was prepared by spreading a slurry of mixing LFP powders, carbon black and polyvinylidene fluoride (PVDF) binder (dissolved in NMP) in a mass ratio of 90:5:5 on a piece of Al foil. Then the Al foil was dried under vacuum at 120 °C for 12 h. The loading of LFP is ~8.0 $mg \cdot cm^{-2}$.

2.4. Preparation of electrolytes and test cells assembling

The bare electrolyte was prepared by introducing 1.0 M $LiPF_6$ into ester solvent (EC: DMC: EMC = 1:1:1 (V/V)). 2-Mercaptopyridine (2 $mg \cdot ml^{-1}$) was added into bare electrolyte to prepare the control electrolyte. The 2032-type coin cells using different electrolytes were assembled in a glove box filled with Ar gas ($H_2O < 10^{-7}$, $O_2 < 10^{-7}$). Li || Li symmetrical cells were assembled with two Li foil electrodes. For Li || Li symmetrical cells with dendrites-filled Li foil, the Li || Li cells with new Li foils were cycled in bare electrolyte for 20 cycles at the current density of 1.0 $mA \cdot cm^{-2}$ for dendrites growth. Then, the Li foil electrodes with dendrites were taken down and assembled for Li || Li symmetrical cells again. The LFP or NCM811 cathodes were assembled with Li foil anodes for full cells.

2.5. Electrochemical measurements

Electrochemical performance was tested on battery testing system (Land battery tester, Wuhan, China). The electrochemical workstation (CHI660E, Chenhua Ltd., Shanghai) was employed for electrochemical measurement. The EIS were recorded in the frequency ranging from 100 kHz to 0.01 Hz. The scan rate of CV is 10 $mV \cdot s^{-1}$. The Li || Li symmetrical cells were tested at different current densities and capacities. The Li || Li symmetrical cells with dendrites-filled Li foil were tested at 1.0 $mA \cdot cm^{-2}$/1.0 $mA \cdot h \cdot cm^{-2}$. The LFP full-cells were tested in ester electrolyte at different C-rates in the potential range of 2.5–4.1 V *vs* Li^+/Li. The NCM811 full-cells were tested in ester electrolyte at 1.0C rate in the potential range of 2.5–4.25 V *vs* Li^+/Li.

3. Results and Discussion

Fig. 1(a)–(b) illustrates the deposition process of metallic lithium on pristine substrate. It is well known that the initial dendrites (tips) are always inevitably formed during the initial process due to the inhomogeneity of the local electric field and microenvironment. In the bare ester-based electrolyte, anions and solvent molecules are adsorbed near the surface and eventually decompose to form the SEI film. The SEI film consists of an inorganic inner layer and an organic outer layer on the anode surface, that is, the inner layer is comprised of compact inorganic products (*e.g.*, Li_2CO_3, LiF, Li_2O, *etc.*) with a relatively higher mass density and the outer layer is reduced organic products (*e.g.*, $(CH_2OCO_2Li)_2$, ROLi, $ROCO_2Li$, *etc.*), which has a relatively low density [29]. The inhomogeneous SEI film leads to severe Li dendritic growth and finally results in the failure of the batteries.

In ester-based electrolyte with 2Mpy additive, the molecules of additive are also a part of adsorbed layer as well as solvent molecules [23]. 2Mpy can accelerate Li deposition process as a charge transfer mediator and enable to keep its structure stability without decomposed during cycling. In ester-based electrolyte, the concave surface would shrink and the convex surface would be expanded by deformation with the initial Li tips growth. leading the content increasing of 2Mpy on the concave surface with shrinkage, while the content of 2Mpy on the convex surface reduced. The content change of 2Mpy adsorption results in the different rate of Li deposition on concave or convex surface, the faster Li^+ reduction and deposition occurred on the concave regions. By this way, a smooth surface of lithium deposition finally achieved on the Li metal anode.

The morphology of Li deposition on Cu substrate in different electrolyte were observed by SEM and exhibited in Fig. 1(b) and Figs. S1 and S2. The uneven surface of deposited layer and lithium dendrites with irregular shapes formed in the bare

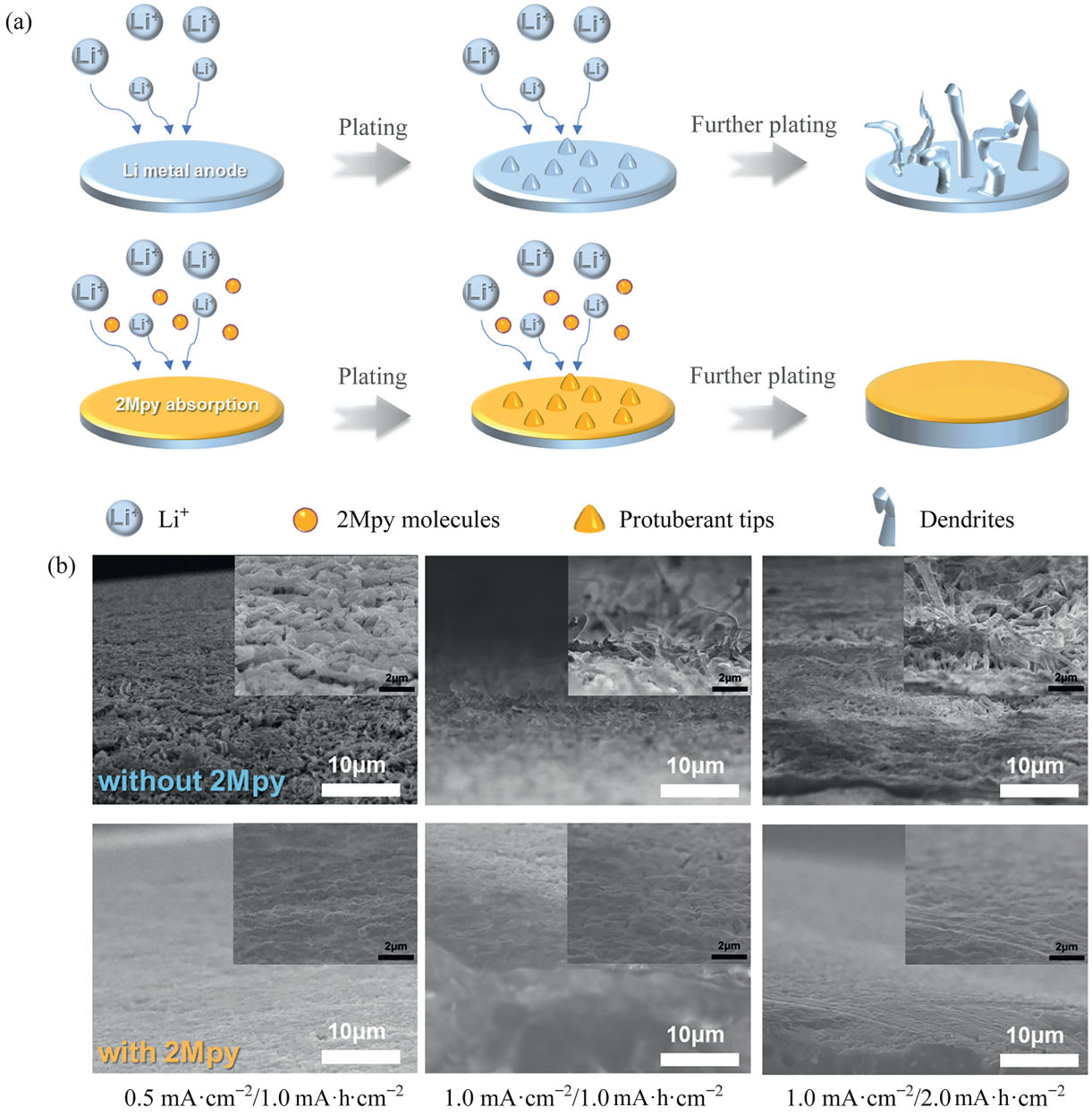

Fig. 1. (a) Schematic illustration of Li metal deposited on substrate in ester-based electrolyte without or with 2Mpy additive. (b) The SEM images of Li metal deposited on Cu substrates with different changeable capacity and current in ester-based electrolyte without or with 2Mpy additive.

electrolyte. The loose deposition of lithium and many voids among the lithium granules are easily noted as well. Compared with ether-based electrolytes, the SEI formed in ester-based electrolytes is more complex and has fewer inorganic components and poorer uniformity, so the growth of dendrites is more serious than the lithium dendritic growth in ether-based electrolytes [23]. Accompanied by the increasing of current density or areal capacity for Li deposition, the Li dendrites become sharper and more severe and a large number of lithium dendrites perpendicular to the deposited layer can be observed, which are the culprit for the short circuit of Li metal batteries. After 2Mpy adding, the surface of Li deposition became denser and the deposition surface became significantly smoother. Despite the increase in current density or areal capacity, the surface of the lithium deposited layer remains smooth.

The electrochemical performance of Li metal anode in ester-based electrolyte with or without 2Mpy are further verified by Li || Li symmetrical cells, as shown in Fig. 2(a) and S3. The sharply drop of over potential was observed after about 150 cycles for the Li || Li symmetrical cells in electrolyte without 2Mpy at 1.0 $mA \cdot cm^{-2}$/1.0 $mA \cdot h \cdot cm^{-2}$, while, the frequent voltage fluctuations appeared when the current density increased to 2.0 $mA \cdot cm^{-2}$, the which could be explained by the repeated formation/fracture of SEI and the continuous Li dendrites growth. On contrast, the symmetrical cells go through stable cycling in ester-based electrolyte with 2Mpy additive, benefited from its mechanism of accelerating deposition process promoted filling up the concave regions leading to the leveling effect on Li metal anode. As a result, a stable Li plating/stripping cycling can maintain over 650 h at 1.0 $mA \cdot cm^{-2}$/1.0 $mA \cdot h \cdot cm^{-2}$, accompanying with a low over-potential of ~90 mV. And the performance of a symmetrical cells with 2Mpy in electrolyte are still better than that with none at 2.0 $mA \cdot cm^{-2}$/1.0 $mA \cdot h \cdot cm^{-2}$.

Moreover, the morphology of Li metal anodes after different cycles under 1.0 or 2.0 mA·cm^{-2} was compared, respectively corresponding to the cycling performance on the left. Obviously, Li deposition during the Initial cycle is inhomogeneous. Many protrusions appeared after first cycle at 1.0 mA·cm^{-2} in ester-based electrolyte without 2Mpy adding, as shown in Fig. 2(b) and S4. It can be observed that irregular dendrites gathered on the surface of Li anodes. After 20 cycles of rapid plating/stripping of metallic Li, thicker layer consisted of Li dendrites covered up the anode surface. After 150 cycles, these sharp Li dendrites may penetrate the separator and result in cell short circuit which is reflected in the time-potential curve in Fig. 2(a). After 2Mpy additive was introduced into ester-based electrolyte, although still some uneven area appeared on the surface of Li metal electrode, the surface is smoother than it in bare electrolyte. Along with the continuous cycling, the Li metal electrode maintained a flat surface without Li dendrites throughout 20 cycles. The electrode still keeps a dendrite-free surface after 150 cycles of Li plating/stripping. When the current density increased to 2.0 mA·cm^{-2}, similar law of morphological changes can be concluded form the SEM images of Li metal anodes after different cycles. The Nyquist plots of the electrochemical impedance spectroscopy of Li||Li symmetrical cells at different cycles were exhibited in Fig. S3. The impedance reduced after long-term cycling, The symmetrical cell with 2Mpy additive present smaller impedance than that of the bare one, which can be attributed to healthy electrode/electrolyte interface without dendrites' damage. To prove the efficacy of 2Mpy in improving reversibility under different C-rate cycling, a series of plating/stripping measurements were performed under elevated current densities of 0.5, 1.0, 2.0, 4.0, 2.0, 1.0 and 0.5 mA·cm^{-2} with areal capacity of 1.0 mA·h·cm^{-2} of the Zn reversibly cycled (Fig. 2(d)). The Li || Li symmetrical cell with 2Mpy shows a more stable voltage profile with a smaller plating/stripping over-potential at each C-rate than symmetrical cell without 2Mpy adding.

To eliminate the uncertainty related to the substrate surface, a method based on pre-plating and final stripping Li has been reported to calculate the average CE [30,31]. Firstly, a given amount of charge (Q_T) is used to deposit Li onto the Cu substrate. Secondly, a smaller portion of this charge (Q_C) is used to cycle Li for n cycles. Finally, an exhaustive strip of the remaining Li reservoir is performed. The final stripping charge (Q_S), corresponding to the quantity of Li remaining after cycling, is measured. The average CE over *n* cycles can be calculated follow the equation:

$$CE_{average} = \frac{nQ_C + Q_S}{nQ_C + Q_T}$$

As is shown in Fig. 2(d), an average CE of the Cu || Li cell with 2Mpyreaches 87.02% at a current density of 1.0 mA·cm^{-2}, which is much higher than that of cells without (70.50%). The better reversibility of Li plating/stripping can be realized *via* 2Mpy introducing.

Meanwhile, the Li foils with dendrites covered, which have already gone through 20 cycles under 1.0 mA·cm^{-2}, were used for evaluate the effect of additive to further investigate the morphology evolution of Li deposition with the participation of 2Mpy (Fig. S6). The dendrites grown more severe than before after cycled in original ester-based electrolyte, but healed themselves and finally achieved flat surface of Li metal anode in electrolyte with 2Mpy additive. This is can be attributed to the faster Li^+ deposition on concave regions than it on convex regions *via* more amount of 2Mpy adsorption [32].

Fig. 3(a)–(b) and S7 exhibit the XPS analysis of the anodes surface after 20 cycles in ester-based electrolyte without or with 2Mpy. The inorganic LiF, and organic products from reduced ester solvent molecules (*e.g.* $(CH_2OCO_2Li)_2$, ROLi, $ROCO_2Li$, *etc.*), can be observed on the surface after cycled [33–35]. It should be noted that no extra components of N or S element appeared on the surface of anode after 2Mpy introduced into electrolyte. the specific

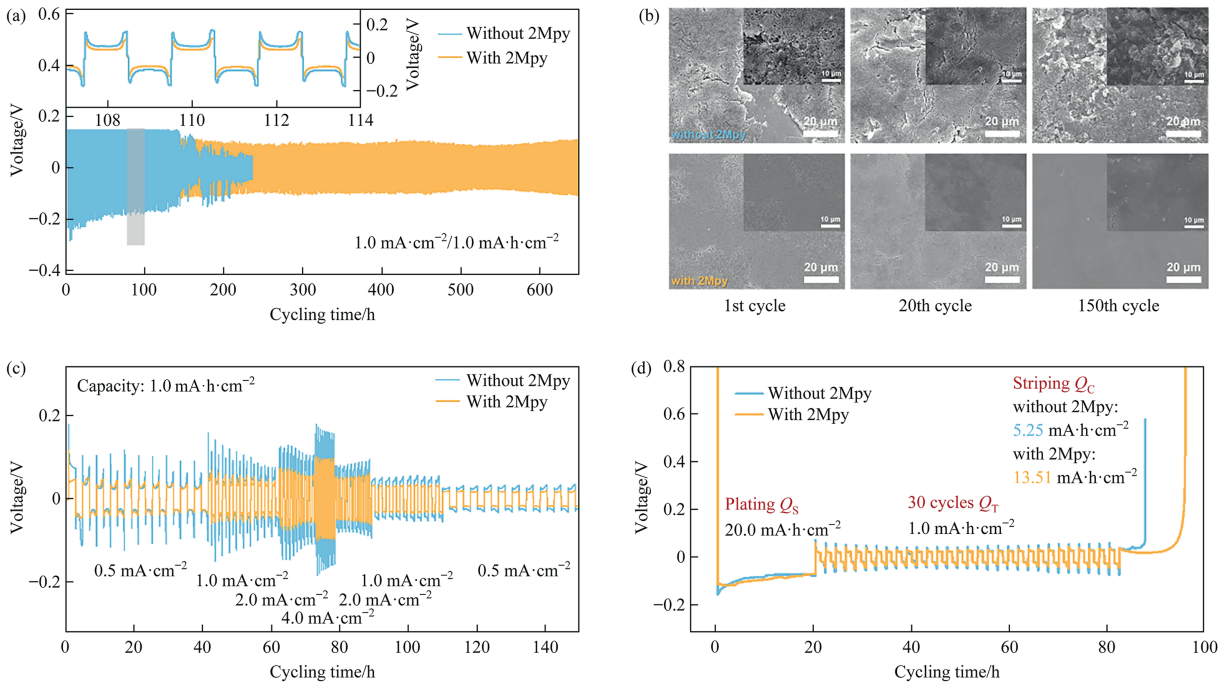

Fig. 2. (a) The Li || Li symmetrical cells in different ester-based electrolytes at 1.0 mA·cm^{-2}/1.0 mA·h·cm^{-2}. Insert: detailed analysis of voltage profiles among 100 cycles. (b) The SEM images of Li metal anodes of Li || Li symmetrical cells after 1, 20 and 150 cycles under 1.0 mA·cm^{-2}/1.0 mA·h·cm^{-2}, respectively. (c) The C-rate performance of Li || Li symmetrical cells in different ester-based electrolytes. (d) Voltage-time curves to calculate the average coulombic efficiency of Cu || Li half cells with and without the 2Mpy additive at 1.0 mA·cm^{-2}. The capacity of pre-plated Li is 20.0 mA·h·cm^{-2}, the cycling capacity is 1.0 mA·h·cm^{-2}.

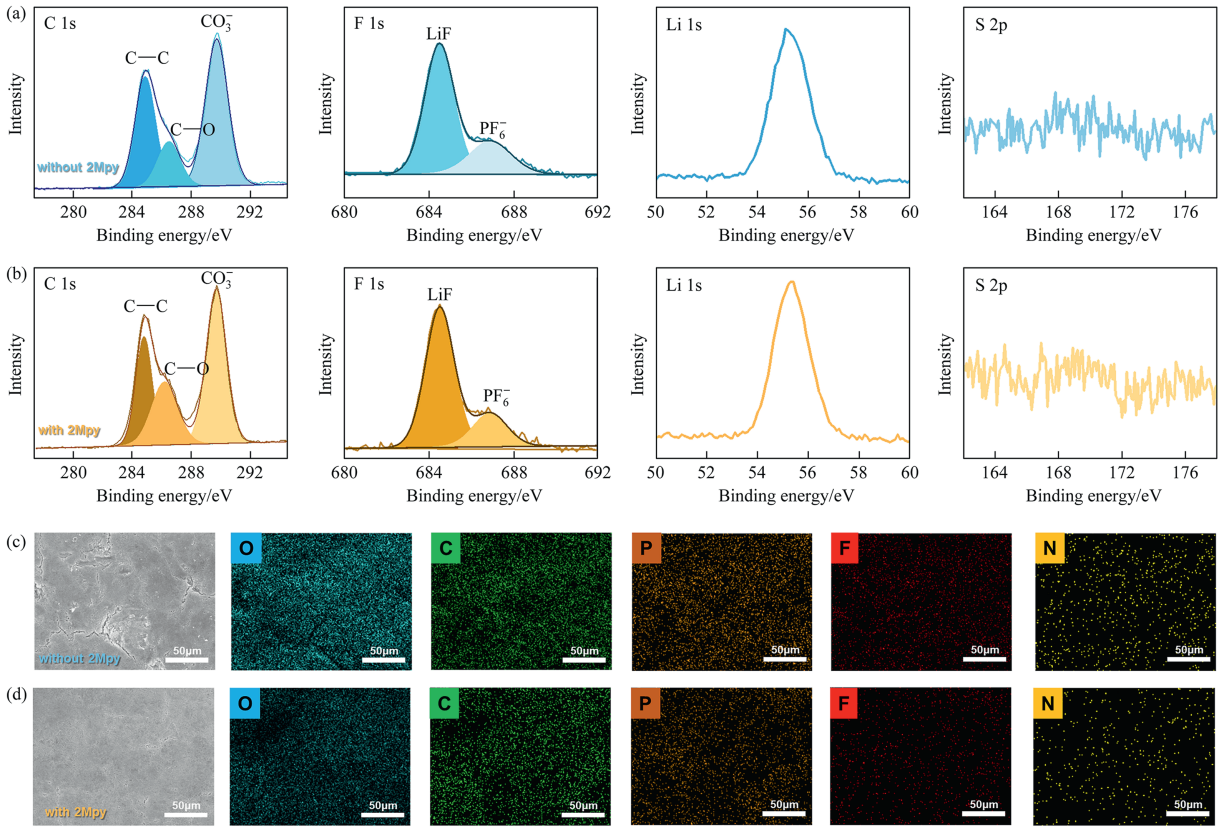

Fig. 3. (a, b) The XPS analysis of Li foil after 20 cycles in ester-based electrolyte without or with 2Mpy; (c, d) The elemental mapping of the Li foil after 20 cycles in ester electrolyte without or with 2Mpy.

peaks shown in N 1s and S 2p spectrum of Li metal anode cycled in ester-based electrolyte with 2Mpy added are similar to these in bare ester-based electrolyte. According to the elements mapping shown in Fig. 3(c),(d), the same conclusion can be inferred that 2Mpy additive can keep stable during the deposition process of metallic Li and does not participate in the formation of SEI.

The electrochemical cyclic voltammetry (CV) was also employed to investigate the Li plating/stripping behaviors (Fig. S8). The redox peaks in the voltage region among −0.5 – 0.7 V corresponded to the Li depositing (negative scan) and stripping (positive scan) reactions. Without additive in electrolyte, the peak current (I_P) was 20 mA corresponding to peak potential (U_P) of 0.529 V. After introducing 2Mpy into electrolyte, a higher I_P (23.5 mA) and lower U_P (0.505 V) can be observed was 0.28 V, indicating a better kinetic of Li redox benefiting from 2Mpy.

As we furtherly investigated, although the LUMO energy level of 2Mpy is lower than that of ether solvent molecules [36,37], which makes 2Mpy molecules more likely to accept electrons, it can remain stable after accepting electrons thanks to the overall conjugated structure of 2Mpy. The lower LUMO energy level makes it easier for electrons to transfer into the 2Mpy molecule and transfer it to Li^+ to maintain the electrical neutrality of the molecule, acting as a charge transfer mediator and promoting the lithium deposition reaction. Here, the HOMO and LUMO energy levels of 2Mpy are compared with those of ester or ether solvent molecules, as shown in Fig. 4(a). It was able to be inferred that the

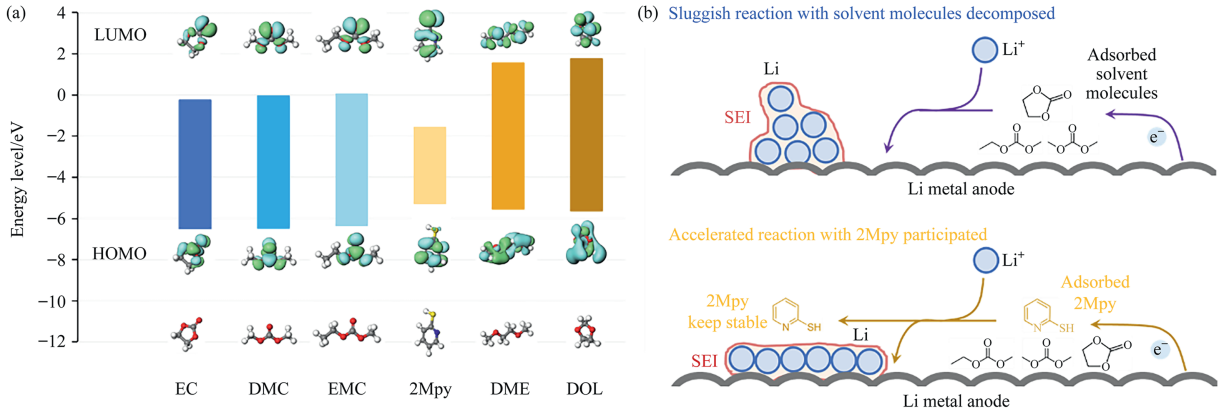

Fig. 4. (a) The energy level of ester solvent molecules, 2Mpy additive and ether solvent molecules; (b) the Schematic illustration of Li deposition without or with 2Mpy additive participated.

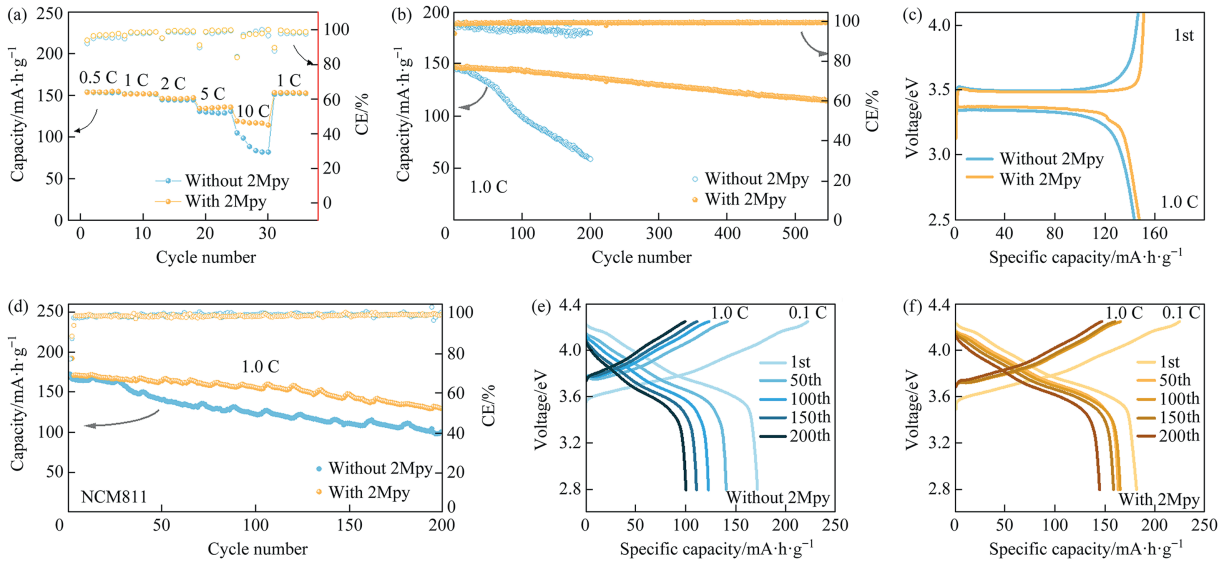

Fig. 5. (a) the C-rate performance and (b) Long-term cycling performance of $LiFePO_4$||Li full cells in ester-based electrolyte without or with 2Mpy. (c) Voltage–capacity curves of $LiFePO_4$||Li full cells at 1.0C. (d) Long-term cycling performance of NCM811||Li full cells in ester-based electrolyte without or with 2Mpy. (e, f) Voltage–capacity curves of NCM811||Li full cells of different cycles.

same regular rule can be extended to ester-based electrolyte. In short, whether it is ether-based electrolyte or ester-based electrolyte, a similar process of 2Mpy participating in the lithium deposition occurs (Fig. 4(b)), in which charge transfer mediator additive of 2Mpy can adsorbed on anode surface and promote charge transfer at the Li metal/electrolyte interface [38], rather than decomposing like the original adsorbed ester solvent molecules such as EC, DMC or EMC, resulting in slow lithium deposition.

$LiFePO_4$||Li and NCM811||Li full-cells were also assembled to evaluate the performance of the 2Mpy additive. As shown in Fig. 5(a), the specific capacity of Li||$LiFePO_4$ using a bare ester-based electrolyte decreased when the C-rate increased from 0.5 to 10.0C. In particular, the capacity decays significantly in only 6 cycles in just 6 cycles under 10.0C. On the contrary, in electrolyte with 2Mpy, the $LiFePO_4$||Li cell presented increased specific capacity at high C-rates and the specific capacity can recover well when current density returned to 1.0 C. As demonstrated in Fig. 5(b)–(c), the specific capacity of Li||$LiFePO_4$ cell in bare electrolyte exhibited a continuous decay, which may cause by uncontrollable dendrites growth and repeated fragmentation and formation of SEI leading to the adverse reaction between metallic Li and ester-based electrolyte. However, with 2Mpy additive, the $LiFePO_4$||Li cell has a smaller polarization in its first cycle and performed a stable cycling with average coulombic efficiency of 99.53% over 1000 cycles at 1.0 C. For NCM811||Li full-cells, the specific capacity improved with 2Mpy introducing into ester-based electrolyte (Fig. 5(d)). The reason was able to infer form the polarization curve of each cycle, as shown in Fig. 5(e)–(f). The additive significantly reduced the increase in polarization of NCM811||Li full cell, which may be due to the participation of 2Mpy in achieving a smooth and dendrite-free electrode/electrolyte interface, thereby reducing the side reactions of the electrolyte.

4. Conclusions

In summary, we have developed application of a universal 2Mpy additive for ester-based electrolyte and achieve long-term cycling of lithium metal batteries. The 2Mpy enable to achieve dendrite-free surface by accelerating Li redox as a charge transfer mediator, and keeping stable during long-term cycling, finally a smooth and uniform anode surface can be achieved. This kinds of additive with stable conjugated structure can work in ester-based electrolyte, and enhance the performance of Li metal anode for practical application. We believe that this unique additive can advance the realization of safe and high-performance lithium metal batteries.

CRediT Authorship Contribution Statement

Tianyi Zhou: Writing – review & editing, Writing – original draft, Project administration, Methodology, Investigation, Funding acquisition, Formal analysis. Lin Hu: Investigation. Qichen Lu: Investigation. Peng Liu: Methodology. Ruling Huang: Formal analysis. Bo Hu: Software. Panxing Bai: Methodology. Shaorong Duan: Resources. Xiaofan Pin: Formal analysis. Rong Liu: Software. Kexin Zhang: Project administration. Xiaoxu Sun: Data curation. Yidan Wang: Investigation. Yaoyu Li: Methodology. Yujia Zhang: Investigation. Yi Yan: Resources. Peng Jiang: Writing – review & editing. Henghui Zhou: Writing – review & editing. Xiaolong Wang: Writing – review & editing.

Declaration of Competing Interest

The authors declare that they have no known competing financial interests or personal relationships that could have appeared to influence the work reported in this paper.

Acknowledgements

This research was supported by China Huaneng Group Technology Project (HNKJ24-HF16).

Supplementary Material

Supplementary data to this article can be found online at https://doi.org/10.1016/j.cjche.2025.09.034.

References

[1] L.F. Xiao, Z.Q. Zeng, X.W. Liu, Y.J. Fang, X.Y. Jiang, Y.Y. Shao, L. Zhuang, X.P. Ai, H.X. Yang, Y.L. Cao, J. Liu, Stable Li metal anode with "ion–solvent-coordinated" nonflammable electrolyte for safe Li metal batteries, *ACS Energy Lett.* 4 (2) (2019) 483–488.

[2] M.M. Tao, J.N. Chen, H.X. Lin, Y.G. Zhou, D.H. Zhao, P.Z. Shan, Y.T. Jin, Y. Yang, Recent advances in quantifying the inactive lithium and failure mechanism of Li anodes in rechargeable lithium metal batteries, *J. Energy Chem.* 96 (2024) 226–248.

[3] Y.F. Hu, Z.C. Li, Z.P. Wang, X.L. Wang, W. Chen, J.C. Wang, W.W. Zhong, R.G. Ma, Suppressing local dendrite hotspots *via* current density redistribution using a superlithiophilic membrane for stable lithium metal anode, *Adv. Sci. (Weinh)* 10 (12) (2023) e2206995.

[4] M. Nangir, A. Massoudi, H. Omidvar, Surface modification of the Li metal anode by alloying, aliphatic, viscoelastic, and Li-M-X ternary systems towards Li dendrite suppression, *J. Power Sources* 624 (2024) 235532.

[5] X.D. Lin, L. Li, E. Lora da Silva, T. Yang, Q.X. Liu, Emerging macromolecular brush-based materials for stabilizing lithium metal anodes, *Mater. Today* 77 (2024) 19–38.

[6] X.Y. Liu, J. Li, Y.C. Xiao, X.C. Dong, L. Tao, Z.Y. Liu, Z. Liu, J. Zhang, S.J. Xu, The MOFs derived Co, Zn co-doping porous carbon framework as the collector for stable Li metal anodes, *Colloids Surf. A Physicochem, Eng. Aspects* 702 (2024) 135112.

[7] Z.Y. Yu, Y.Y. Gu, Q. Sun, Y. Zheng, Y.F. Zhang, M.M. Zhang, D.L. Zhang, Z.J. Zhang, Y. Jiang, Research progress of modified metal current collectors in sodium metal anodes, *Chin. Chem. Lett.* 36 (6) (2025) 109997.

[8] J.W. Qiu, R.L. Qiu, Z.Y. Mao, Y. Han, P. Madhusudan, X. Wang, C. Wang, C.S. Qi, X. Yu, S.Z. Zeng, D.J. Fu, P.G. Han, S.Z. Niu, A review on copper current collector used for lithium metal batteries: challenges and strategies, *J. Energy Storage* 100 (2024) 113683.

[9] T.Y. Zhou, Y.L. Mu, J.Y. Wu, B. Zhong, C.K. Yang, Q. Wang, W. Liu, H.H. Zhou, P. Jiang, Interwoven nickel(II)-dimethylglyoxime nanowires in 3D nickel foam for dendrite-free lithium deposition, *Chin. Chem. Lett.* 33 (4) (2022) 2165–2170.

[10] S.H. Pan, S. Nachimuthu, B.J. Hwang, G. Brunklaus, J.C. Jiang, Synergistic dual electrolyte additives for fluoride rich solid-electrolyte interface on Li metal anode surface: mechanistic understanding of electrolyte decomposition, *J. Colloid Interface Sci.* 649 (2023) 804–814.

[11] Z. Wang, B. Al Alwan, K.Y. Simon Ng, Multi-functions of amino thiophenol additives for shielding lithium metal anode in advanced Li-S battery, *Mater. Sci. Eng. B* 297 (2023) 116727.

[12] D.Q. Huang, C.H. Zeng, M.H. Liu, X.R. Chen, Y.H. Li, S.J. Hu, Q.C. Pan, F.H. Zheng, Q.Y. Li, H.Q. Wang, Introducing KI as a functional electrolyte additive to stabilize Li metal anode, *Chem. Eng. J.* 454 (2023) 140395.

[13] X.T. Li, Z.H. Fu, J. Wang, X.H. Zhao, Y.K. Zhang, W.Z. Liu, Q. Cai, C. Hu, Dilithium phthalocyanine as electrolyte additive for the regulation of ion solvation and transport towards dendrite-free Li metal anodes, *Chem. Eng. J.* 450 (2022) 138112.

[14] T.Y. Zhou, Y.L. Mu, L. Chen, D.X. Li, W. Liu, C.K. Yang, S.B. Zhang, Q. Wang, P. Jiang, G.L. Ge, H.H. Zhou, Toward stable zinc aqueous rechargeable batteries by anode morphology modulation *via* polyaspartic acid additive, *Energy Storage Mater.* 45 (2022) 777–785.

[15] T.Q. Xiang, Z.Y. Hu, H. Huo, J.J. Zhou, L. Li, Tailoring the electronic conductivity of coating layer on the composite separator for Li metal anode, *Electrochim. Acta* 511 (2025) 145394.

[16] W.Z. Nan, B.T. Li, S.J. Yan, S.L. Dai, Dynamic interface layer enables epitaxial Li deposition for anode-free Li metal batteries, *J. Phys. Chem. Solid.* 196 (2025) 112350.

[17] Z.W. Chen, Y.R. Xu, Y.X. Song, L.Y. Chen, J.S. Wang, M. He, J.H. Luo, X.Z. Ma, J. Xiong, J.G. Xu, W. Yao, Robust porous artificial layers with boosted lithiophilicity and Li+ diffusion for dendrite-free Li metal anodes, *J. Power Sources* 615 (2024) 235105.

[18] B. Li, P.Y. Yan, M.M. Jia, L. Wang, Y.R. Qiao, H.W. Li, C.H. Wu, Z.Z. Zhang, D.M. Dai, D.H. Liu, Engineering lithiophilic LiC_x layer to robust interfacial chemistry between LAGP and Li anode for Li-metal batteries, *Chin. Chem. Lett.* 36 (7) (2025) 110145.

[19] Y. Zhang, X. Lou, J. Dan, C. Franke, L. Tang, J. Li, Z. Gao, L. Zhou, B. Chen, T. Li, T. Liu, Coupling alloyed lean lithium anodes with PIM-1-blended PEO electrolytes synergistically promotes reversible Li stripping/deposition reactions for all-solid-state lithium-metal batteries, *J. Energy Storage* 94 (2024) 112399.

[20] K. Kisu, S. Kim, H. Oguchi, N. Toyama, S.I. Orimo, Interfacial stability between $LiBH_4$-based complex hydride solid electrolytes and Li metal anode for all-solid-state Li batteries, *J. Power Sources* 436 (2019) 226821.

[21] A.N. Wang, M.Y. Yi, S.L. Chang, H.B. Shi, Y.L. Xiao, Y.T. Hu, J.Q. Zheng, Y.Q. Lai, M.R. Wang, Z.A. Zhang, Regulating Li deposition behavior at anodic interface induced by SbF_3 electrolyte additive in all-solid-state Li metal batteries, *Chem. Eng. J.* 474 (2023) 145593.

[22] T.Y. Zhou, R.C. Xu, X. Cao, J.T. Zhang, J.Y. Wang, R.L. Huang, X.F. Ping, P.X. Bai, Z.T. Sun, M.Y. Liu, X.L. Wang, Bio-inspired rigid-soft coupling gel polymer electrolyte for stable lithium batteries, *Sci. China Mater.* 67 (7) (2024) 2256–2265.

[23] T.Y. Zhou, D.H. Shi, Q. Wang, C.K. Yang, X.L. Wang, K. Wu, Y.L. Mu, J.Y. Wu, Z. Y. Liu, W. Liu, H.H. Zhou, P. Jiang, Accelerating Li^+/Li redox through the regulation of the electric double layer for efficient lithium metal anodes, *Chem. Eng. J.* 468 (2023) 143676.

[24] Z.H. Lin, Q.B. Xia, W.L. Wang, W.S. Li, S.L. Chou, Recent research progresses in ether- and ester-based electrolytes for sodium-ion batteries, *InfoMat* 1 (3) (2019) 376–389.

[25] X. Kang, Electrolytes and interphases in Li-ion batteries and beyond, *Chem. Rev.* 114 (23) (2014) 11503–11618.

[26] P.B. Lai, B.Y. Huang, X.D. Deng, J.L. Li, H.M. Hua, P. Zhang, J.B. Zhao, A localized high concentration carboxylic ester-based electrolyte for high-voltage and low temperature lithium batteries, *Chem. Eng. J.* 461 (2023) 141904.

[27] R.G. Xu, Q. Liu, Q. Yang, W. Yang, D.B. Mu, C.L. Li, L. Li, R.J. Chen, F. Wu, Study on carbonate ester and ether-based electrolytes and hard carbon anodes interfaces for sodium-ion batteries, *Electrochim. Acta* 462 (2023) 142787.

[28] A.K. Huang, Z. Ma, P. Kumar, H.H. Liang, T. Cai, F. Zhao, Z. Cao, L. Cavallo, Q. Li, J. Ming, Low-temperature and fast-charging lithium metal batteries enabled by solvent-solvent interaction mediated electrolyte, *Nano Lett* 24 (2024) 7499–7507.

[29] C. Hou, J.H. Han, P. Liu, C.C. Yang, G. Huang, T. Fujita, A. Hirata, M.W. Chen, Operando observations of SEI film evolution by mass-sensitive scanning transmission electron microscopy, *Adv. Energy Mater.* 9 (45) (2019) 1902675.

[30] B.D. Adams, J.M. Zheng, X.D. Ren, W. Xu, J.-G. Zhang, Accurate determination of coulombic efficiency for lithium metal anodes and lithium metal batteries, *Adv. Energy Mater.* 8 (7) (2018) 1702097.

[31] Y.L. Mu, T.Y. Zhou, D.X. Li, W. Liu, P. Jiang, L. Chen, H.H. Zhou, G.L. Ge, Highly stable and durable Zn-metal anode coated by bi-functional protective layer suppressing uncontrollable dendrites growth and corrosion, *Chem. Eng. J.* 430 (2022) 132839.

[32] Q. Wang, C.K. Yang, J.J. Yang, K. Wu, C.J. Hu, J. Lu, W. Liu, X.M. Sun, J.Y. Qiu, H. H. Zhou, Dendrite-free lithium deposition *via* a superfilling mechanism for high-performance Li-metal batteries, *Adv. Mater.* 31 (41) (2019) e1903248.

[33] S.T. Oyakhire, H.X. Gong, Y. Cui, Z.N. Bao, S.F. Bent, An X-ray photoelectron spectroscopy primer for solid electrolyte interphase characterization in lithium metal anodes, *ACS Energy Lett.* 7 (8) (2022) 2540–2546.

[34] B.P. Thapaliya, T. Wang, A.Y. Borisevich, H.M. Meyer III, X.-G. Sun, M.P. Paranthaman, C.A. Bridges, S. Dai, *In situ* ion-exchange metathesis induced conformal LiF surface films on cathode (NMC811) as a cathode electrolyte interphase, *Adv. Funct. Mater.* 33 (44) (2023) 2302443.

[35] Y.Z. Liu, X.Y. Meng, Y. Shi, J.S. Qiu, Z.Y. Wang, Long-life quasi-solid-state anode-free batteries enabled by Li compensation coupled interface engineering, *Adv. Mater.* 35 (42) (2023) e2305386.

[36] H.R. Cheng, Q.J. Sun, L.L. Li, Y.G. Zou, Y.Q. Wang, T. Cai, F. Zhao, G. Liu, Z. Ma, W. Wahyudi, Q. Li, J. Ming, Emerging era of electrolyte solvation structure and interfacial model in batteries, *ACS Energy Lett.* 7 (1) (2022) 490–513.

[37] Z.L. Ye, S.J. Xie, Z.Y. Cao, L.P. Wang, D.X. Xu, H. Zhang, J. Matz, P. Dong, H.Y. Fang, J.F. Shen, M.X. Ye, High-rate aqueous zinc-organic battery achieved by lowering HOMO/LUMO of organic cathode, *Energy Storage Mater.* 37 (2021) 378–386.

[38] J.F. Lei, Y.Q. Zhang, Y.X. Yao, Y. Shi, K.L. Leung, J. Fan, Y.C. Lu, An active and durable molecular catalyst for aqueous polysulfide-based redox flow batteries, *Nat. Energy* 8 (12) (2023) 1355–1364.